Global Change Biology

Global Change Biology (2010), doi: 10.1111/j.1365-2486.2010.02245.x

Direct effects of temperature on forest nitrogen cycling revealed through analysis of long-term watershed records

E. N. JACK BROOKSHIRE*[1,2], STEFAN GERBER*[2], JACKSON R. WEBSTER†, JAMES M. VOSE‡ and WAYNE T. SWANK‡

*Department of Ecology and Evolutionary Biology, Princeton University, Princeton, NJ 08544, USA, †Department of Biological Sciences, Virginia Polytechnic Institute and State University, Blacksburg, VA, USA, ‡USDA Forest Service, Coweeta Hydrologic Laboratory, Otto, NC, USA

Abstract

The microbial conversion of organic nitrogen (N) to plant available forms is a critical determinant of plant growth and carbon sequestration in forests worldwide. In temperate zones, microbial activity is coupled to variations in temperature, yet at the ecosystem level, microbial N mineralization seems to play a minor role in determining patterns of N loss. Rather, N losses often appear to vary with seasonality in hydrology and plant demand, while exports over longer periods are thought to be associated with increasing rates of anthropogenic N deposition. We analyzed long-term (21–32 years) time series of climate and stream and atmospheric chemistry from two temperate deciduous forest watersheds in the southeastern USA to understand the sensitivity of internal forest N cycles to climate variation and atmospheric deposition. We evaluated the time series with a simple analytical model that incorporates key biotic constraints and mechanisms of N limitation and cycling in plant–soil systems. Through maximum likelihood analysis, we derive biologically realistic estimates of N mineralization and its temperature sensitivity (Q_{10}). We find that seasonality and long-term trends in stream nitrate (NO_3) concentrations can in large part be explained by the dynamics of internal biological cycling responding to climate rather than external forcing from atmospheric chemistry. In particular, our model analysis suggests that much of the variation in N cycling in these forests results from the response of microbial activity to temperature, causing NO_3 losses to peak in the growing season and to accelerate with recent warming. Extrapolation of current trends in temperature and N deposition suggests that the upturn in temperature may increase future N export by greater than threefold more than from increasing deposition, revealing a potential direct effect of anthropogenic warming on terrestrial N cycles.

Keywords: climate variation, ecosystem model, forest nitrogen cycling, long-term data, nitrogen deposition, nitrogen mineralization, small watershed, temperature sensitivity

Received 12 March 2010; revised version received 12 March 2010 and accepted 2 April 2010

Introduction

Variations in climate have the potential to affect the balance of atmospheric nitrogen (N) input and hydrologic loss that controls long-term ecosystem productivity. Although large anthropogenic N inputs to land ecosystems have been shown to induce N saturation and leaching of excess plant-available N to ground and stream waters (Aber *et al*., 2002), most N uptake by forest plants is thought to be supplied by microbial mineralization of detrital N to plant-available forms (Likens & Bormann, 1995). The terrestrial N cycle is expected to respond to climate variation as key steps in the cycle are mediated by temperature- and moisture-dependent microbial reactions which, in turn, regulate the immediate availability of N to plants (Schlesinger, 1997; Gruber & Galloway, 2008). Theoretical considerations (Davidson & Janssens, 2006; Manzoni & Porporato 2007), soil–core incubations (Knoepp & Swank, 2002; Knoepp & Vose, 2007), and plot-scale warming experiments (Rustad *et al*., 2001; Melillo *et al*., 2002) indicate high climate sensitivity of N mineralization but results have been difficult to scale to whole forests and multiannual time periods and often do not fully integrate effects of plant uptake and ecosystem inputs and losses.

Temporal patterns of N concentration and flux in small watersheds can provide important insights into terrestrial N cycling and its sensitivity to climate variation and external perturbation (Bormann & Likens, 1967). In particular, many temperate forests show seasonal and long-term trends in stream N chemistry, but disentangling the multiple and often covarying effects

[1]Present address: E. N. Jack Brookshire, Department of Land Resources and Environmental Sciences, Montana State University, Bozeman, MT 59717, USA.

[2]These authors contributed equally to this work.

Correspondence: E. N. Jack Brookshire, e-mail: jbrookshire@montana.edu

of N deposition, hydrology, and disturbance from potential climate signatures remains an important challenge (Aber *et al.*, 2002). In humid temperate forests, climate is characterized by seasonal swings in temperatures that can be up to 50 °C, a range that is much larger than recent and projected rates of warming. This seasonal range encompasses temperatures over which microbial activity and thus mineralization varies up to an order of magnitude (Knoepp & Swank, 2002; Knoepp & Vose, 2007). Despite strong temperature effects on microbial activities, direct expression of seasonality in mineralization is not observed at the ecosystem level across many humid forests of the northeastern USA, Canada, and northern Europe where concentrations and losses of nitrate (NO_3) in stream waters tend to peak during winter and early spring and decline to baseline levels during summer (Likens & Bormann, 1995; Anderson & Lepistö, 1998; Spoelstra *et al.*, 2001; Elliott *et al.*, 2002). This classical pattern has been attributed to flushing of inorganic N during spring snow melt, sometimes in combination with freeze–thaw cycles in soils, and declines in plant N uptake (Likens & Bormann, 1995). However, in warmer temperate latitudes, winters are less severe and thus mechanisms explaining stream chemistry in cooler forests may not predict patterns of NO_3 loss (Mulholland, 2004). In fact, streams draining warm temperate forests often show NO_3 concentration peaks in summer (Swank & Vose, 1997; Mulholland, 2004; Goodale *et al.*, 2009).

Recently, several studies have made use of climate and chemical time series from small watershed forests (e.g., Mitchell *et al.*, 1996; Park *et al.*, 2003; Rogora *et al.*, 2008; Sebestyen *et al.*, 2009) to investigate climate sensitivity of N losses, but inference has largely been based on correlation analysis of drivers which often show similar trends and are thus difficult to disentangle. In contrast, ecosystem models have also been developed to investigate N cycling in small watershed forests (e.g., Aber *et al.*, 1997; Hong *et al.*, 2005). Ecosystem models incorporate an integrated and process-based representation of biogeochemical cycles in forested watersheds and the comprehensive character of these models allows, in principle, mechanistic attribution of biogeochemical cycles to global change drivers. Although process-based models are useful tools to interpret stream chemistry, they often require a substantial array of data for local parameterization, and such data exists only for a very few sites.

Here, we use a mechanistic but highly reduced and analytically tractable ecosystem model to evaluate unique long-term (21–32 years) measurements of climate and water chemistry in forest watersheds at the Coweeta Hydrologic Laboratory (CHL) in North Carolina, USA. Our objective was to disentangle effects of atmospheric deposition and climate variation on temporal patterns of N loss from CHL watershed ecosystems. We use maximum likelihood estimation (MLE) to infer values for a small set of ecosystem parameters and then explore the sensitivity of our model to central parameters. We use our model findings to discuss potential mechanisms as to why CHL and other forests display summer rather than winter–spring peak NO_3 concentrations. Finally, we use the model to explore mechanisms through which global change may affect future patterns of N loss from CHL forests.

Methods

Field methods

CHL is a USDA Forest Service experimental watershed and a National Science Foundation Long-Term Ecological Research Site (Swank & Vose, 1997). Stream concentrations and fluxes of dissolved inorganic N (DIN) at CHL are exceptionally low relative to deposition, a pattern likely reflecting N-limited plant growth and N accumulation in wood and soils (Swank & Vose, 1997). Mean annual precipitation at CHL is plentiful ($180\,cm\,yr^{-1}$ at $\sim$700 m elevation; $230\,cm\,yr^{-1}$ at $\sim$1200 m), well distributed (no seasonal drought), and falls primarily as rain (only 2–10% as snow). We analyzed data from a low- (WS14; 992 m) and high-elevation (WS36; 1542 m) watershed of mixed-oak and northern hardwood forest types, respectively. Streams were monitored continuously for discharge (Q) and sampled weekly for chemistry at V-notch weirs with samples aggregated into volume-weighted monthly values. Precipitation was collected on a weekly basis for chemistry and volume weighted to obtain monthly values. All samples were analyzed for ammonium (NH_4) and NO_3 following Swank & Vose (1997). We calculated monthly values of bulk deposition and dissolved inorganic exports based on volume-weighted concentrations. Long-term mean inorganic N deposition rates were 6.1 and $7.2\,kg\,N\,ha^{-1}\,yr^{-1}$ for low- and high-elevation watersheds, respectively. Stream chemistry data for WS14 were missing for the 1974–1980 period (due to weir replacement) and we therefore analyze this time series for the 1981–2001 period. The time period analyzed for WS36 was 1972–2003.

Model development and analysis

We developed an ecosystem model that incorporates key mechanisms of terrestrial N cycling known to be sensitive to climate variation and which is rooted in established biogeochemical models (Raich *et al.*, 1991; Rastetter *et al.*, 2001; Gerber *et al.*, 2010). We then evaluated observations based on MLE by fitting monthly data and model to obtain optimal parameter values. The model describes the change with time of NH_4 (A) and NO_3 (N) in soils as a series of linear relationships

$$\frac{dA}{dt} = \frac{1}{h}\left(\overline{M} r_T r_D + D_A\right) - As\left(\overline{k_{NIT}} r_T r_D + k_L + k_P\right), \qquad (1)$$

$$\frac{dN}{dt} = \frac{D_N}{h} + As\overline{k_{NIT}}r_T r_D - N(k_L + k_P), \quad (2)$$

where $\bar{M}$ is the long-term mean of the mineralization rate, D_A and D_N are deposition rates for NH_4 and NO_3, respectively, h the depth range of the active soil, $\overline{k_{NIT}}$ is a nitrification rate constant, and k_L and k_P are sink rates of A and N through leaching and biological removal, respectively. Further, r_T and r_D are modifiers that consider effects of soil temperature and soil moisture, respectively, and s is a sorption coefficient that considers the reduced mobility of NH_4 in soils (Matschonat & Matzner, 1995). A enters the system from microbial mineralization M and bulk atmospheric deposition D_A. N is formed during nitrification of A or added as deposition D_N. Removal of both A and N are modeled based on time varying first-order kinetics representing internal sinks (plants, microbes, nitrification) or hydrologic losses. For simplicity, inputs are homogenously distributed over a soil volume to the depth h. Although deposition rates are measured quantities, we approximate dynamics of mineralization by determining its long-term mean value $\bar{M}$ as a parameter and applying a climate modifier that varies with temperature and soil moisture where the temperature sensitivity is a Q_{10} function

$$r_T = Q_{10}^{(T-\bar{T})/10}, \quad (3)$$

where T is the temperature and $\bar{T}$is its long-term average. The moisture modifier (r_D) is parameterized based on Q and is assumed to follow a Gaussian curve that allows increase of saturation and decrease of biotic processes, mimicking moisture limitation at low soil moisture levels and possible oxygen limitations at high levels of soil wetness

$$r_D = \exp\left[-\frac{(k_L - \mu)^2}{\sigma}\right]\phi, \quad (4)$$

where μ and σ are shape parameters representing optimal value and sensitivity in the soil moisture function, respectively. We require the long-term average of the product of r_T and r_D to be 1, hence

$$\phi = \frac{n}{\sum_i \left\{ Q_{10}^{(T_i-\bar{T})/10} \exp\left[-\frac{(k_{L,i}-\mu)^2}{\sigma}\right]\right\}}, \quad (5)$$

where n is the number of observations through time. The drainage rate coefficient k_L is calculated with $\frac{Q}{h}$, where Q is runoff in length units. The uptake rate k_p denotes an internal sink strength to reflect first-order plant and microbial immobilization. We approximated the nitrification rate k_{NIT} to have the same temperature and moisture modifier as mineralization. Production and sinks of A and N are treated similar as in other process-based biogeochemical models (Parton *et al*., 1993; Aber *et al*., 1997; Rastetter *et al*., 1997). Three critical approximations lead to the analytical framework presented in Eqns (1) and (2): First, hydrology is not modeled but rather soil moisture conditions and drainage rates are inferred from data. Second, we assume the system to be perpetually N-limited with a plant/microbial sink strength k_p constant through time. In other words, plant/microbial demand is always greater than supply and the uptake machinery (e.g., root exploitation of soils, plant–mycorrhizal interactions) and thus the N removal capacity (per unit A or N) does not change through time. We later discuss implications for our model of relaxing this assumption (i.e., allowing k_p to vary with climate). Third, we approximate mineralization through the combination of its long-term mean state and perturbation caused by temperature and soil moisture. This last approximation can be justified by relatively small changes of soil N stocks over the time considered (Swank & Vose, 1997). Implicit to the model setup is also the assumption that microbial dynamics adjust without lag to environmental drivers (temperature and soil moisture), which can be justified by fast microbial turnover ($\sim$days). Turnover times of mineral forms of N in soils are fast ($\sim$1 day; Stark & Hart, 1997) and therefore levels of N equilibrate rapidly compared with changes in the driving variables. This allows the assumption of steady state $\left(\frac{dN}{dt} = \frac{dA}{dt} = 0\right)$ for each monthly time step, resulting in

$$\hat{A}_i = \frac{\bar{M}r_{T_i}r_{D_i} + D_{A,i}}{hs\left(\overline{k_{NIT}}r_{T_i}r_{D,i} + k_{L,i} + k_P\right)}, \quad (6)$$

$$\hat{N}_i = \frac{hs\overline{k_{NIT}}r_{T_i}r_{D,i}A_i + D_{N,i}}{h\left(k_{L,i} + k_P\right)}. \quad (7)$$

where $\hat{A}_i$ and $\hat{N}_i$ are the steady-state NH_4 and NO_3 concentrations for a particular month i in the time series. We further assume equivalency between stream water and soil solutions, which is supported empirically in heavily shaded and low productivity CHL streams (Brookshire *et al*., 2009).

We used MLE to constrain the small set of parameters (k_p, $\overline{k_{NIT}}$, h, s, $\bar{M}$, Q_{10}, μ, σ) and the γ-distribution to allow for nonnormal error distribution (similar to Ise & Moorcroft, 2006). The likelihood L for the species s representing A or N measured in month i was calculated as follows:

$$L(s,i) = \frac{D_{s,i}^{a_s-1}}{b^{a_s}\Gamma(a_s)}\exp\left(-\frac{D_{s,i}}{b_s}\right), \quad (8)$$

where a and b are parameters for the gamma function Γ, and have a different value for A and N, and $D_{s,i}$ the absolute difference between modeled and observed values

$$D_{s,i} = \left|Y_{s,i}(\text{predicted}) - Y_{s,i}(\text{observed})\right|, \quad (9)$$

where $Y_{s,i}$ represents modeled or simulated A or N in month i. The parameters were given a large *a priori* range (Table 1). The best model fit (i.e., best choice of parameters) is achieved when the sum of the log-transformed likelihood (l) is maximized

$$l = \sum_s \sum_i \log[L(s,i)]. \quad (10)$$

We used MATLAB (R2007a, version 7.4.0.287) functions *fmincon* and *gamfit* to estimate best model fit of model parameters and the parameters of the γ-distribution, respectively. Upper and lower constraints of parameters for the optimization are given in Table 1.

The results of our base model [Eqns (6) and (7)] were compared with reduced versions with no sensitivity to moisture ($r_D = 1$), no temperature sensitivity ($Q_{10} = 1$), no mineralization, and to a null model where A and N are estimated

Table 1 Range (Lower and Upper bounds) of parameter values used in randomizations and parameter results of maximum likelihood estimation

Parameter	$\bar{M}$ (kg N ha^{-1} yr^{-1})	Q_{10}	μ (year^{-1})	σ (year^{-2})	h (m)	s	k_P (month^{-1})	K_{NIT} (month^{-1})	MLE
Lower bound	0	10^{-6}	0.01	0.01	0.05	0	–	–	–
Upper bound	400	10	3000	3000	1	1	–	–	–
WS36									
$\bar{M}$low	84.8	1.7	–	–	0.50	0.66	78.5	246	8811.1
$\bar{M}$free	176	2.2	–	–	0.49	0.89	156	671	8813.2
WS14									
$\bar{M}$low	29.1	4.0	–	–	0.64	0.71	31.6	77	5957.4
$\bar{M}$free	180	3.0	–	–	0.14	0.95	776	2793	5959.4

Results for μ and σ are not presented as the model was determined to be insensitive to soil moisture. $\bar{M}$ low represents optimized parameter values using fixed minimum values of $\bar{M}$ whereas $\bar{M}$ free represents results where all parameters including $\bar{M}$ were allowed to vary freely in likelihood estimations.
MLE, maximum likelihood estimation.

based on their long-term mean. The test statistics for comparison of those nested models is given by

$$-2[l(\mathbf{p}_1) - l(\mathbf{p}_2)] \sim \chi^2, \quad (11)$$

where $l(\mathbf{p}1)$ and $l(\mathbf{p}2)$ are the maximum likelihood of the models with the parameter set $\mathbf{p}_1$ and $\mathbf{p}_2$, respectively (Burnham & Anderson, 1998). The degree of freedom for the χ^2 test is the difference in the number of parameters used in the models under evaluation. Tests with the Matlab optimization procedure showed sensitivity of the 'best estimate' to the first 'guess' of the parameters, indicating that the iterations converged on a local maximum of the likelihood function. We therefore performed a Monte Carlo simulation with 1000 random draws, where the first guess is randomly chosen within the range given in Table 1 assuming a continuous uniform distribution. We estimated confidence intervals for the key parameters for Q_{10} and $\bar{M}$ based on Monte Carlo simulations: Q_{10} (and in a separate Monte Carlo procedure $\bar{M}$) was a random draw from the range given in Table 1 and subsequently held constant for the MLE, while all the other parameters were optimized to obtain the best fit. This process was repeated 1000 times to obtain l for a specific choice of Q_{10} or $\bar{M}$. The Akaike information criterion (AIC) (Akaike, 1974) given by AIC = $2p-2l$, where p is the number of parameters, served as measure of whether a particular choice of Q_{10} or $\bar{M}$ was plausible. We followed Burnham & Anderson (1998) who suggest that differences from optimum AIC of approximately 4–7 correspond roughly to 95% confidence interval.

We explored the sensitivity of the model to long-term changes in detail by calculating future (30 years) N export rates given the observed increase in bulk N deposition and temperature. We extrapolated the trends in deposition based on linear regression of monthly data and constructed future temperature as a combination of the mean and linear trend in temperature for each month. Future discharge was assumed to be the mean of the observation period, as there was no significant trend in the data sets. To estimate future DIN exports, we first used the optimum parameter set (Table 1) for the two watersheds and either included or disregarded deposition rates. We then picked the parameter set from the Monte Carlo simulations that remained within the confidence interval of the optimal fit but also resulted in the smallest possible contribution of the internal cycle to the long-term trend in N exports, relative to the effects of increasing N deposition.

Results

Observed losses of NO_3 and NH_4 from both CHL watersheds remained low over the entire study period (Fig. 1a and b). NO_3 concentrations dominated DIN over NH_4. NH_4 concentrations were always near detection levels and exhibited little consistent temporal variation. Stream NO_3 concentrations exhibit distinct seasonality with maxima occurring during summer months and low values during autumn and winter. The long-term record at CHL (since 1970) shows significant (linear regression; $P<0.001$) increases in temperature (annual: 0.043 °C yr^{-1}; winter: 0.07 °C yr^{-1}), N deposition (0.084 kg N ha^{-1} yr^{-2}), and concentrations and losses of NO_3 (0.005 kg N ha^{-1} yr^{-2}) while water fluxes (precipitation and runoff) show no trend.

The optimization procedure revealed distinct temperature dependence of temporal patterns of N loss from CHL forests: for both watersheds, Q_{10} values were distinctly different from 1 ($P<0.001$). In fact, seasonal variation in stream NO_3 was to a large degree explained by the dynamics of mineralization (Fig. 1c) which closely tracked fluctuations in temperature (Fig. 2). For both watersheds, frequency distributions and associated γ-distributions for deviations in DIN show that our model explains a considerable amount of the variation in monthly stream DIN concentrations (model−data vs. data−mean data; Fig. 3). The model fit resolved 26% and 59% (R^2) of the total variation in NO_3 concentrations and

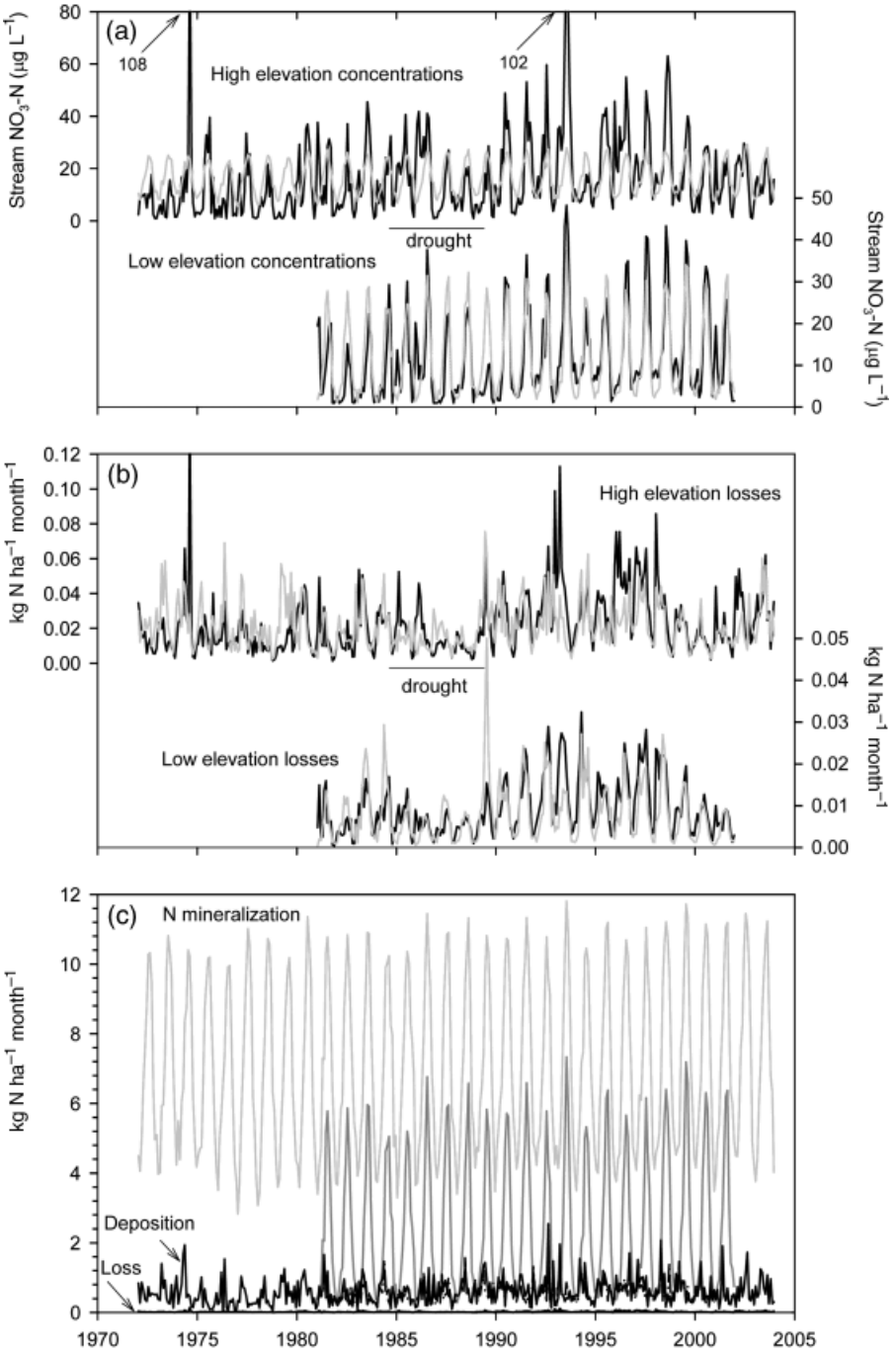

Fig. 1 Temporal patterns of (a) stream nitrate (NO_3) concentrations, (b) inorganic ($NO_3 + NH_4$) nitrogen (N) export, and (c) N inputs from mineralization and atmospheric deposition for high- (WS36) and low-elevation (WS14) Coweeta Hydrologic Laboratory (CHL) reference watersheds. Observations are black lines and model simulations are gray lines. (c) WS36 is the light gray and WS14 is dark grey line. Mineralization time series were generated using the conservative estimate of minimum $\bar{M}$ determined from 1000 Monte Carlo simulations while optimizing (maximum likelihood estimation, MLE) for the other parameters.

72% and 89% of variation in mean monthly concentrations for high- and low-elevation watersheds. Mismatches in the temporal distribution of NO_3 between model and observations possibly reflect aspects of microbial/plant uptake and/or hydrology not captured in our model, particularly in the high-elevation watershed. Overall, however, our simple model appears to capture the major temporal patterns of N losses.

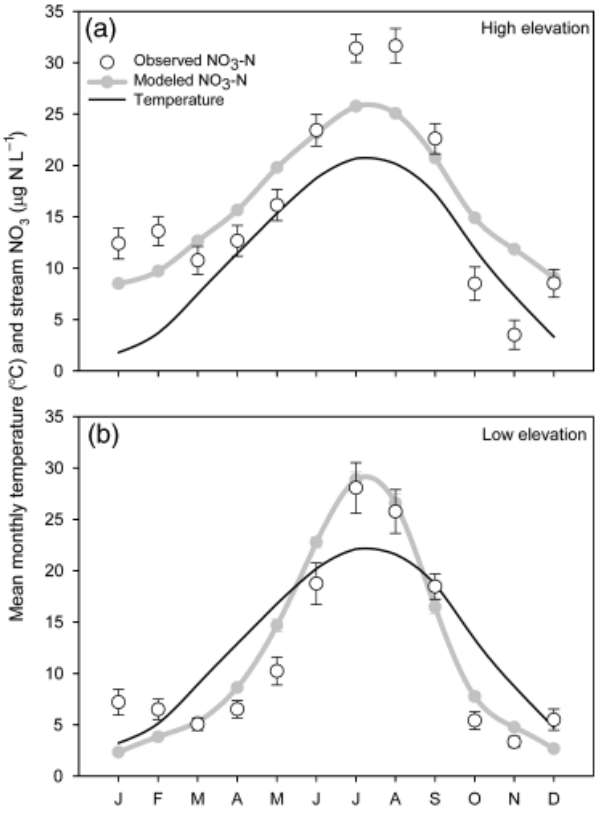

Fig. 2 Climatology of stream nitrate (NO_3) concentrations for the (a) high-elevation and (b) low-elevation Coweeta Hydrologic Laboratory (CHL) watersheds. Circles are the long-term observed mean monthly NO_3 concentration (±1SE), gray lines are mean simulated monthly NO_3 concentration (±1SE), and black lines are mean monthly air temperatures.

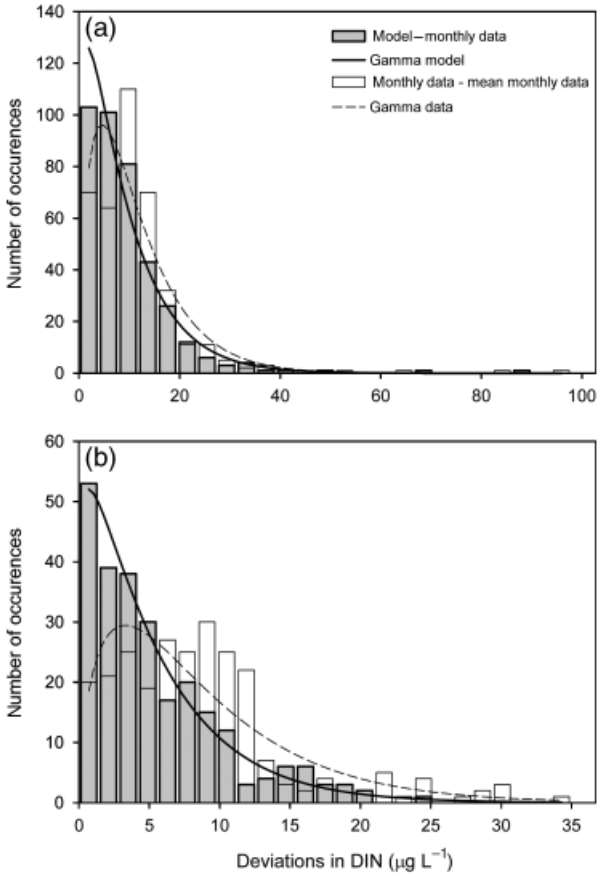

Fig. 3 Frequency distribution of the deviations in monthly dissolved inorganic nitrogen (DIN) concentration for the (a) high-elevation and (b) low-elevation watershed. We calculated absolute deviations between the model estimate and monthly data (thick gray bars) and between the long-term mean and monthly data (thin transparent bars). The lines denote the fitted γ-distribution for model deviation (thick line) and data variation (thin line).

The maximum likelihood method constrained likely values (Burnham and Anderson cutoff = 4; Table 1) of Q_{10} for mineralization between 1.7–2.3 and 2.7–4.0 for high- and low-elevation watersheds (Fig. 4a). We found optimal mineralization fluxes of 180 kg N ha^{-1} yr^{-1} at both sites but $\bar{M}$ was poorly constrained at its upper limit (Fig. 4b). However, based on the Burnham cutoff, values of mineralization below 29 and 85 kg N ha^{-1} yr^{-1} for the lower and higher watershed are outside the confidence interval and thus incompatible with observed stream concentrations. We found higher estimates of $\bar{M}$ at high elevation, despite slightly cooler temperatures. This pattern results from the fact that the mean state of M in the model is not a function of climate perturbations but rather reflects long-term N cycling rates. However, we note that the difference in $\bar{M}$ between the two watersheds (Fig. 4b) was not statistically significant.

In contrast to temperature responses, we found that MLE did not change significantly ($P = 0.72$ and 0.98; maximum likelihood ratio test) when the soil moisture parameter (r_D) was omitted from the model, suggesting little sensitivity of soil moisture on M. Soil moisture effects appear not to be obscured by covariation of runoff with temperature because moisture sensitivity remained unimportant even after omitting temperature dependence in the model. An alternative version of our model with separate temperature and moisture parameters for M and k_{NIT} also showed no difference in MLE ($P > 0.99$) from the results presented here. However, the absence of soil moisture dependency in our analysis might partly be caused by the parameterization of moisture through runoff. Further, there was unexplained variability in NO_3 concentrations and fluxes, particularly in the high-elevation watershed where modeled output was dampened compared with observations.

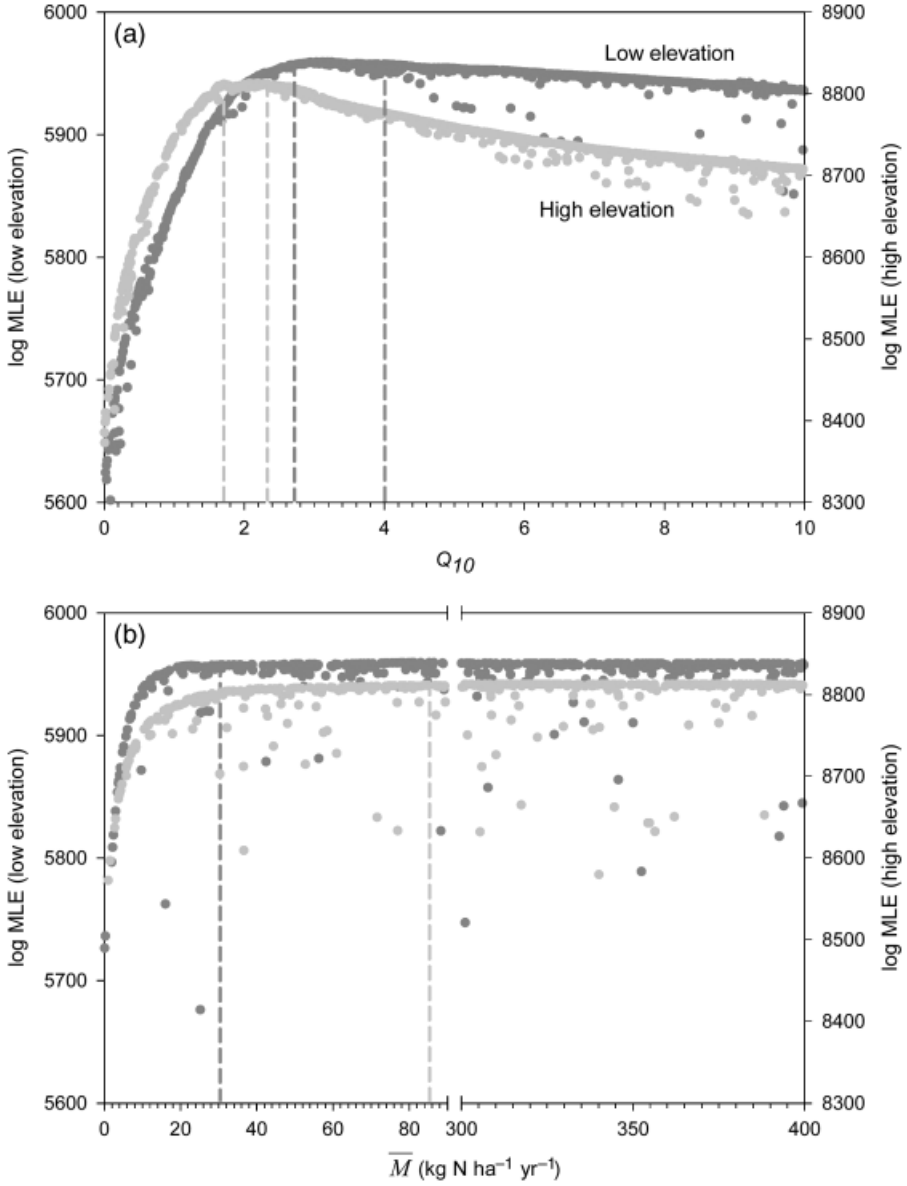

Fig. 4 Maximum likelihood estimation (MLE) of parameters (a) Q_{10} and (b) $\bar{M}$ for high elevation (light gray circles) and low elevation (dark gray circles). Simulations were run 1000 times using randomly drawn fixed values of Q_{10} and $\bar{M}$ while optimizing for the other parameters, showing that optimal values of Q_{10} are well constrained while $\bar{M}$ is not constrained at the upper limits. Vertical lines indicate optimal ranges (within approximately 5%) of Q_{10} and minimum values of $\bar{M}$.

The explained variation in NO_3 was lower for N exports ($R^2 = 39$–54%) compared with concentrations, showing the effect of drainage rates on fluxes. However, the model analysis also indicates that dilution of the available N pool is minimal because the internal sink strength is considerably stronger (i.e., $k_P \gg k_L$) and thus replenishment of the N pool is considerably faster (i.e., $M \gg k_L N$) than drainage rates. Therefore, high DIN concentrations obtained during summer months result from high mineralization rates and not a decline in base flow discharge.

Our model projections of DIN exports revealed a dominant influence of the increasing temperature trend vs. N deposition in shaping future DIN exports (Fig. 5). The calculated trends in export rates range between 6.3×10^{-4} and 8.9×10^{-4} kg ha^{-1} yr^{-2} for the low-elevation watershed and between 9.7×10^{-4} and 12.8×10^{-4} kg ha^{-1} yr^{-2} for the high-elevation watershed. For all scenarios, we found that the fractional contribution of N deposition {[1- (no dep trend/dep trend) $\times$ 100]; Fig. 5} never exceeded a maximum of 24% to the overall trend in DIN export.

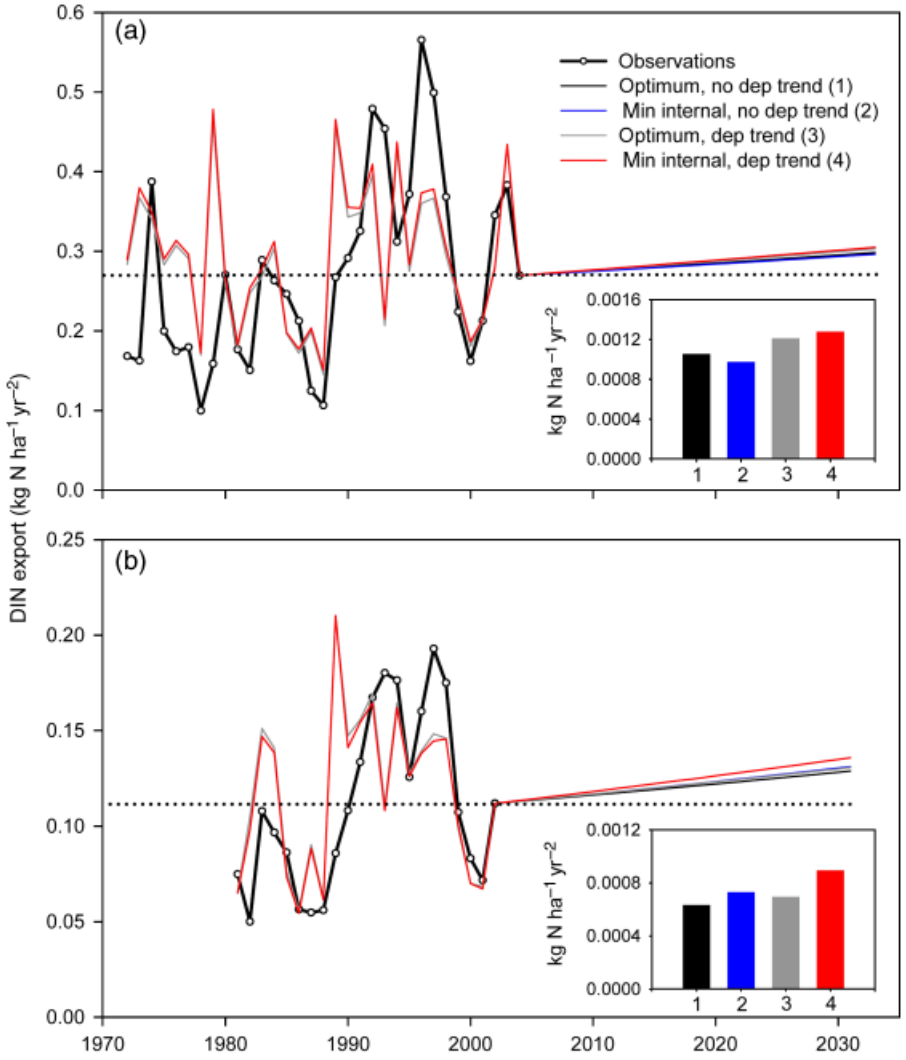

Fig. 5 Annual dissolved inorganic nitrogen (DIN) losses for the observation period and modeled projection 30 years in the future for (a) high-elevation and (b) low-elevation Coweeta Hydrologic Laboratory (CHL) watersheds. Projections were calculated using the observed mean monthly data and monthly trends in temperature and assumptions about annual trends in deposition. The different simulations vary in parameter configuration and include or exclude future trends in N deposition. We first used the optimum parameter set (optimum) for the two watersheds and either included or disregarded deposition rates (dep trend or no dep trend). We then picked the parameter set from the Monte Carlo simulations in Fig. 3 that remained within the confidence interval of the optimal fit but also resulted in the smallest possible fractional contribution of the internal cycle (min internal) to the long term trend in N exports. The model realizations consider the continuation of the historical trend of N deposition into the future (dep trend) or constant future deposition rates according to the mean over the historic period (no dep trend). The inset shows the annual rate of change in DIN export for each of the parameterizations (1–4).

Discussion

Separating the multiple effects of global environmental change on terrestrial systems represents a major scientific challenge given the complexity of biogeochemical cycles and the fact that different vectors of global change are occurring simultaneously (e.g. N deposition, warming, CO_2). Long-term records in combination with process-based evaluations can help to detect, attribute, and understand the response of terrestrial systems to different anthropogenic forcings. Fitting CHLs long-term record to a simple but mechanistic model of terrestrial N cycling enabled us to evaluate the individual sensitivities of these forest ecosystems to effects of climate variation and anthropogenic N deposition.

Most importantly, our parameter optimization confirmed the notion (e.g., Aber *et al.*, 1997) that the internal N sink strength dominates vectors of N losses ($k_P \gg k_L$,

Table 1). It follows that because soil moisture effects did not enhance the predictability of our model, levels of DIN (mostly NO_3) in our analysis can be approximated from Eqns (6) and (7) to be

$$[\mathrm{DIN}] = \frac{\overline{M} m Q_{10}^{(\bar{T}-T)/10}}{h k_p} + \frac{m D_A + D_N}{h k_p}, \qquad (12)$$

where DIN concentrations ([DIN]) are a linear combination of the variability in mineralization (i.e., temperature, first term on the right-hand side of the equation) and deposition (second term of the equation) and m is a unitless modifier ($m = [k_p/s + k_{NIT}]/[(k_p + k_{NIT}]$) that approaches one in our optimization.

Over a seasonal cycle, the variations in mineralization are large compared with the seasonality in deposition [Figs 1 and 2; first vs. second term of the right-hand side of Eqn (12)]. Concentrations and losses are therefore strongly driven by the temperature dependence of mineralization. Here, we parameterized mineralization based on a long-term $\bar{M}$ combined with a Q_{10} function. The optimization procedure selected for high rates of mineralization to accommodate the distinct seasonal cycle of higher NO_3 concentrations in summer and lower concentrations during the dormant season. The fitted $\bar{M}$ was thus sufficiently large to dilute the imprint of N deposition on DIN losses. An additional increase in $\bar{M}$ did not further improve the model prediction, resulting in a leveling off of the likelihood l in Fig. 4. The fitting exercise overall correctly reproduced rates of mineralization in excess of observed rates of N deposition. Our minimum estimates of internal N generation (29–85 kg N ha^{-1} yr^{-1}; Table 1) were 5–15 times higher than inputs from deposition and were similar to measures of N fluxes from litter fall and net mineralization in CHL forests (Elliott *et al*., 2002; Knoepp *et al*., 2008). Optimal levels (180 kg N ha^{-1} yr^{-1}), however, were closer to expected gross mineralization (Stark & Hart, 1997). In addition, although the difference in $\bar{M}$ between lower and higher elevations was not significant in our model, field evidence for lower C:N in litterfall and soils (Brookshire *et al*., 2007; Knoepp *et al*., 2008), and results from soil mineralization assays (Knoepp & Swank, 2002) support the tendency in our results towards higher rates of mineralization in the higher elevation watershed. Similarly, values of Q_{10} found through our model analysis (1.7–4) differed between the two watersheds but were within the average range of Q_{10} for many biological processes including litter decomposition (Davidson & Janssens, 2006) and mineralization determined from local soil incubations (Knoepp & Swank, 2002; Knoepp & Vose, 2007). Further, our finding that internal sources dominate over deposition is broadly consistent with field isotope studies showing that most stream NO_3 derives from nitrification (e.g., Spoelstra *et al*., 2001; Goodale *et al*., 2009).

In our model, the internal sink strength (parameter k_p) does not vary temporally and does not differentiate between plants and other pathways of immobilization. While in our model like in natural forests, plant uptake fluxes vary considerably throughout the year depending on soil N availability, there is in fact little known about how N sink *capacities* (i.e., k_p) might vary through time in natural terrestrial ecosystems. In N-limited forests, plants efficiently remove available N during the growing season (Likens & Bormann, 1995; Swank & Vose, 1997). Yet, our results indicate that a strong internal sink persists regardless of temperature, suggesting that the pattern observed at CHL is driven by the supply of DIN via mineralization. The k_p obtained through optimization reflects the observation that internal sinks draw down NO_3 and NH_4 levels drastically such that DIN exports remain exceedingly low. The idea that microbes and plants have the capacity to effectively out-compete hydrology in times of high N demand is integral to biogeochemical models. In these models the plant and microbial uptake rate constants are set high (Reuss & Innis, 1977; Rastetter *et al*., 1997; Gerber *et al*., 2010) and in some cases, it is even assumed that microbes and plants remove available N completely when N-limited, leaving nothing to hydrological pathways (i.e. $k_p -> \infty$, Aber *et al*., 1997; Thornton *et al*., 2007). Little is known about the temperature sensitivity of N uptake capacities. Raich *et al*. (1991) use an exponential function for plant uptake that corresponds to a Q_{10} value of 1.9. Modifying the internal sink strength with a Q_{10} function would expand k_p as follows:

$$k_p = \bar{k}_p^* Q_{10,k_p}^{(\bar{T}-T)/10}, \qquad (13)$$

where $\bar{k}_p$ is the long-term mean of the internal sink strength. Relaxing the earlier assumption of a constant sink capacity, and instead varying k_p as exponential function of temperature would modify the DIN concentration [substitute Eqn (13) into (12)]:

$$[\mathrm{DIN}] = \frac{m\bar{M}}{h\bar{k}_p} q_{10}^{(\bar{T}-T)/10} + \frac{m D_A + D_N}{h k_p Q_{10}^{(T-\bar{T})/10}}, \qquad (14)$$

where q_{10} represents the quotient of the temperature sensitivity of mineralization and the internal sink strength ($q_{10} = Q_{10}/Q_{10,k_p}$). In this case, the obtained model fit for Q_{10} would in fact represent q_{10}, an *apparent* Q_{10}. A temperature-dependent internal sink thus implies an even higher temperature sensitivity of mineralization. For example, by applying Raich *et al*.'s (1991) Q_{10,k_p} of 1.9 we would obtain Q_{10} for mineralization of 3.2–4.4 and 5.1–7.6 for the higher and lower elevation watersheds, respectively. Instead, the temperature

sensitivities of mineralization and nitrification obtained here are within a biological meaningful range: analysis of functional relationships between temperature and nitrification suggest Q_{10} values of 2.2–2.5 for nitrification (Stark, 1996), and decomposition models use temperature modifiers that are equivalent to Q_{10} values of 1.9–3.2 (Rodrigo *et al*., 1997). It is thus less likely that a strong and consistent change in the internal sink capacity over a seasonal cycle is offsetting an even larger temperature sensitivity of mineralization/nitrification. As an exception, however, levels of DIN are drawn down sharply in November, which is likely caused by increases in N immobilization after leaf abscission (Valett *et al*., 2008). Overall, the consistently low levels of DIN in CHL streams, in combination with peak concentration during the growing season, suggests that to a first approximation, the seasonality in stream NO_3 is driven by DIN supply. That is, DIN concentration tracks the annual cycle of mineralization which, in turn, is shown to be sensitive to temperature variability. The seasonal pattern observed at CHL differs with observations in northern forests of high DIN concentrations in winter and spring. The northern streams' low DIN concentrations in summer have been attributed to enhanced biological uptake strength in times of vigorous growth (Likens & Bormann, 1995), such that the winter–summer difference is the result of biological N demand. These findings would suggest that dormant season retention might vary between cold and warm temperate forests possibly through plant rooting/uptake strategies, N diffusion in soils or feedbacks in plant–microbe interactions that might vary as a function of climate.

We also found that fast replenishment of the soil DIN pool through internal cycling rendered hydrologic dilution/flushing less relevant to the observed stream patterns. That is, while water fluxes do drive DIN exports, concentrations are set almost exclusively by biological mechanisms. However, this might not be true during extreme hydrologic events. In particular, quick-flow runoff has been shown to induce peaks in DIN concentrations in some streams (Sebestyen *et al*., 2009). Our model represents such extreme events insufficiently and is not able to address flushing phenomena or hydrologic flow that might bypass the active soil environment. The model optimization also rendered soil moisture effects on N mineralization to be negligible. We parameterized soil moisture based on monthly runoff while attempting to include water limitation as well as the potential to limit oxygen supply for decomposers. The result from the optimization is in agreement with experimental evidence for weak influences of moisture variation on mineralization in CHL soils (Knoepp & Swank, 2002), while nitrification rates are known to be sensitive to soil moisture (Hong *et al*., 2005; Knoepp & Vose, 2007). However, the presence of soil moisture dependency cannot be ruled out. In combination with fast-adjusting microbial dynamics, high-frequency changes in hydrologic conditions could create export patterns which cannot be resolved with the framework here, but may contribute to some of the unexplained variability in losses. Yet, it should be noted that soil moisture dynamics and its effect on biological activities poses considerable challenges to any biogeochemistry model (see Ise & Moorcroft, 2006).

Biological temperature dependence in our model emerges from the distinct seasonal pattern of NO_3 concentrations observed at CHL. This pattern apparently occurs regardless of forest successional status, persisting during rapid tree growth following clear-cutting in experimental CHL watersheds (Worrall *et al*., 2003) and in nearby old-growth forests (Clinton *et al*., 2003). However, there exist other mechanisms by which stream NO_3 may peak during summer months that our analysis does not address. In particular, in addition to increases in mineralization and nitrification during summer (see Goodale *et al*., 2009), it has been suggested that this pattern results from a combination of (1) seasonal downward shifts in hydrologic flow paths in which NO_3-bearing water bypasses N-immobilizing surface soil horizons and (2) seasonal shifts in in-stream processing particularly during autumn (e.g., Mulholland, 2004; Goodale *et al*., 2009). Our analysis cannot rule out these effects. In fact, the degree of fit – particularly in the high-elevation dataset – suggests that other processes in addition to soil N biogeochemistry are likely operating. Further, we do not address the potential contribution of gaseous losses to NO_3 levels and the observed seasonal pattern, as these cannot be constrained by the available record. Although denitrification may also increase with mean annual or seasonal temperature (Schaefer & Alber, 2007), this loss pathway is not expected to be high under conditions of low N availability and N limitation such as in reference CHL watersheds (Davidson & Swank, 1986). While our results are most consistent with higher nitrification during warm months, we do not see temperature dependence as mutually exclusive of the other explanations. Rather, we offer temperature dependence as a 'first-order' alternative or complimentary hypothesis to these. We suggest, however, that any general explanation of the seasonal pattern must be capable of distinguishing the seasonality of microbial N production and immobilization, plant uptake, N limitation, and hydrologic dynamics and how and why these vary in strength across temperate forests. Our approach thus might offer a simple mechanistic formulation which can be introduced into more detailed representations of watershed nutrient dynamics.

Over the last two decades, a considerable amount of research has focused on the effects of atmospheric N pollution on terrestrial N cycling and loss. More recently, studies have attempted to disentangle the simultaneous effects of atmospheric deposition and climate variation on patterns of N loss from terrestrial ecosystems (e.g., Murdoch *et al*., 1998; Park *et al*., 2003; Watmough *et al*., 2004; Rogora *et al*., 2008; Baron *et al*., 2009). CHL forests show long-term increases in concentrations and exports of NO_3 that parallel increases in temperature and N deposition. On multiyear time scales, rates of N deposition change may contribute to changes in observed N exports. In fact, the two additive terms in Eqn (12) that separate out effects of internal DIN production vs. N deposition have similar magnitudes when the *long-term* trend in temperature and deposition are considered. However, by exploring the parameter space in our model we found that long-term trends in stream N concentrations are overwhelmingly determined by rates of mineralization and its dependence on temperature. Our analysis suggests that warming may be an important driver of future N loss rates from CHL forests. We found that the fractional contribution of N deposition never exceeded a maximum of 24% to the trend in DIN export. Yet, we also note that our calculated trend in DIN export was smaller than the observed change in export over the observational period. Nevertheless, these results emphasize the important role of internal N cycles in shaping ecosystem responses to global change drivers. It is feasible that warming may push the system faster towards saturation than would occur with deposition alone. We emphasize, however, that such threshold behavior of system N saturation is not captured in our reduced form model.

Our results underscore the importance of long-term environmental monitoring in assessing climate–ecosystem dynamics and projected changes. Further, we have shown the utility of and the insights that can be gained through application of simple analytical tools that may extend beyond those provided by correlational analyses. Our analysis of the record of stream chemistry at Coweeta suggests a potentially important role for climate acceleration of local N cycles in affecting long-term patterns of forest productivity and N loss.

Acknowledgements

We thank Susana Bernal for insightful comments on an earlier version of the manuscript. We thank Yiqi Luo and two anonymous reviewers for insightful comments on the manuscript. E. N. J. B. was funded through a grant from the A. W. Mellon Foundation awarded to L. O. Hedin and S. A. Levin. S. G. was funded through a grant from the Cooperative Institute for Climate Science (CICS) awarded to L. O. Hedin.

References

Aber JD, Ollinger SV, Driscoll CT (1997) Modeling nitrogen saturation in forest ecosystems in response to land use and atmospheric deposition. *Ecological Modelling*, **101**, 61–78.

Aber JD, Ollinger SV, Driscoll CT, Likens GE, Holmes RT, Freuder RJ, Goodale CL (2002) Inorganic nitrogen losses from a forested ecosystem in response to physical, chemical, biotic, and climatic perturbations. *Ecosystems*, **5**, 648–658.

Akaike H (1974) A new look at the statistical model identification. *IEEE Transactions on Automatic Control*, **19**, 716–723.

Anderson L, Lepistö A (1998) Links between runoff generation, climate and nitrate–N leaching from forested catchments. In: *Biogeochemical Investigations at the Watershed, Landscape and Regional Scales* (eds Wieder K, Novák M, Černý JV), pp. 227–237. Kluwer Academic Publishers, the Netherlands.

Baron JS, Schmidt TM, Hartman MD (2009) Climate-induced changes in high elevation stream nitrate dynamics. *Global Change Biology*, **15**, 1777–1789.

Bormann FH, Likens GE (1967) Nutrient cycling. *Science*, **155**, 424–429.

Brookshire ENJ, Valett HM, Gerber S (2009) Maintenance of terrestrial nutrient loss signatures during in-stream transport. *Ecology*, **90**, 293–299.

Brookshire ENJ, Valett HM, Thomas SA, Webster JR (2007) Atmospheric N deposition increases organic N loss from temperate forests. *Ecosystems*, **10**, 252–262.

Burnham KP, Anderson DR (1998) *Model Selection and Inference*. Springer Verlag, New York.

Clinton BD, Vose JM, Knoepp JD, Elliott KJ (2003) Stream nitrate response to different burning treatments in Southern Appalachian forests. In: *Proceedings of Fire Congress 2000: The First National Congress on Fire Ecology, Prevention, and Management* (eds Galley KEM, Klinger RC), pp. 174–181. Miscellaneous Publication No. 13, Tall Timbers Research Station, Tallahassee, FL.

Davidson EA, Janssens IA (2006) Temperature sensitivity of soil carbon decomposition and feedbacks to climate change. *Nature*, **440**, 165–173.

Davidson EA, Swank WT (1986) Environmental parameters regulating gaseous nitrogen losses from two forested ecosystems via nitrification and denitrification. *Applied Environmental Microbiology*, **52**, 1287–1292.

Elliott KJ, Boring LR, Swank WT (2002) Aboveground biomass and nutrient accumulation 20 years after clear-cutting a southern Appalachian watershed. *Canadian Journal of Forest Research*, **32**, 667–683.

Gerber S, Hedin LO, Oppenheimer M, Pacala SW, Shevliakova E (2010) Nitrogen cycling and feedbacks in a global dynamic land model. *Global Biogeochemical Cycles*, **24**, 1–15.

Goodale C, Thomas S, Fredriksen G, Elliott E, Flinn K, Butler T, Walter M (2009) Unusual seasonal patterns and inferred processes of nitrogen retention in forested headwaters of the Upper Susquehanna River. *Biogeochemistry*, **93**, 197–218.

Gruber N, Galloway JN (2008) An earth-system perspective of the global nitrogen cycle. *Nature*, **451**, 293–296.

Hong B, Swaney DP, Woodbury PB, Weinstein DA (2005) Long-term nitrate export pattern from Hubbard Brook watershed 6 driven by climatic variation. *Water, Air, and Soil Pollution*, **160**, 293–326.

Ise T, Moorcroft PR (2006) The global-scale temperature and moisture dependencies of soil organic carbon decomposition: an analysis using a mechanistic decomposition model. *Biogeochemistry*, **80**, 217–231.

Knoepp J, Swank W (2002) Using soil temperature and moisture to predict forest soil nitrogen mineralization. *Biology and Fertility of Soils*, **36**, 177–182.

Knoepp J, Vose JM (2007) Regulation of nitrogen mineralization and nitrification in Southern Appalachian ecosystems: separating the relative importance of biotic vs. abiotic controls. *Pedobiologia*, **51**, 89–97.

Knoepp JD, Vose JM, Swank WT (2008) Nitrogen deposition and cycling across an elevation and vegetation gradient in southern Appalachian forests. *International Journal of Environmental Studies*, **65**, 389–408.

Likens GE, Bormann FH (1995) *Biogeochemistry of a Forested Ecosystem*. Springer Verlag, New York.

Manzoni S, Porporato A (2007) A theoretical analysis of nonlinearities and feedbacks in soil carbon and nitrogen cycles. *Soil Biology and Biochemistry*, **39**, 1542–1556.

Matschonat G, Matzner E (1995) Quantification of ammonium sorption in acid forest soils by sorption isotherms. *Plant and Soil*, **168–169**, 95–101.

Melillo JM, Steudler PA, Aber JD *et al*. (2002) Soil warming and carbon-cycle feedbacks to the climate system. *Science*, **298**, 2173–2176.

Mitchell MJ, Driscoll CT, Kahl JS, Likens GE, Murdoch PS, Pardo LH (1996) Climatic control of nitrate loss from forested watersheds in the Northeast United States. *Environmental Science and Technology*, **30**, 2609–2612.

Mulholland PJ (2004) The importance of in-stream uptake for regulating stream concentrations and outputs of N and P from a forested watershed: evidence from long-term chemistry records for Walker Branch Watershed. *Biogeochemistry*, **70**, 403–426.

Murdoch PS, Burns DA, Lawrence GB (1998) Relation of climate change to the acidification of surface waters by nitrogen deposition. *Environmental Science and Technology*, **32**, 1642–1647.

Park J, Mitchell MJ, McHale PJ, Christopher SF, Meyers TP (2003) Impacts of changing climate and atmospheric deposition on N and S drainage losses from a forested watershed of the Adirondack Mountains, New York State. *Global Change Biology*, **9**, 1602–1619.

Parton WJ, Scurlock JMO, Ojima DS *et al*. (1993) Observations and modeling of biomass and soil organic matter dynamics for the grassland biome worldwide. *Global Biogeochemical Cycles*, **7**, 785–809.

Raich JW, Rastetter EB, Melillo JM *et al*. (1991) Potential net primary productivity in South America: application of a global model. *Ecological Applications*, **1**, 399–429.

Rastetter EB, Ågren GI, Shaver GR (1997) Responses of N-limited ecosystems to increased CO_2: a balanced-nutrition, coupled-element-cycles model. *Ecological Applications*, **7**, 444–460.

Rastetter EB, Vitousek PM, Field C, Shaver GR, Herbert D, Ågren GI (2001) Resource optimization and symbiotic nitrogen fixation. *Ecosystems*, **4**, 369–388.

Reuss JO, Innis GS (1977) A grassland nitrogen flow simulation model. *Ecology*, **58**, 379–388.

Rodrigo A, Recous S, Neel C, Mary B (1997) Modelling temperature and moisture effects on C–N transformations in soils: comparison of nine models. *Ecological Modelling*, **102**, 325–339.

Rogora M, Arese C, Balestrini R, Marchetto A (2008) Climate control on sulphate and nitrate concentrations in alpine streams of Northern Italy along a nitrogen saturation gradient. *Hydrology and Earth System Sciences*, **12**, 371–381.

Rustad LE, Campbell JL, Marion GM *et al*. (2001) A meta-analysis of the response of soil respiration, net nitrogen mineralization, and aboveground plant growth to experimental ecosystem warming. *Oecologia*, **126**, 543–562.

Schaefer S, Alber M (2007) Temperature controls a latitudinal gradient in the proportion of watershed nitrogen exported to coastal ecosystems. *Biogeochemistry*, **85**, 333–346.

Schlesinger WH (1997) *Biogeochemistry. An Analysis of Global Change*. Academic Press, San Diego, CA, USA.

Sebestyen SD, Boyer EW, Shanley JB (2009) Responses of stream nitrate and DOC loadings to hydrological forcing and climate change in an upland forest of the northeastern United States. *Journal of Geophysical Research – Biogeosciences*, **114**, 1–11.

Spoelstra J, Schiff SL, Elgood RJ, Semkin RG, Jeffries DS (2001) Tracing the sources of exported nitrate in the Turkey Lakes watershed using $^{15}N/^{14}N$ and $^{18}O/^{16}O$ isotopic ratios. *Ecosystems*, **4**, 536–544.

Stark JM (1996) Modeling the temperature response of nitrification. *Biogeochemistry*, **35**, 433–445.

Stark JM, Hart SC (1997) High rates of nitrification and nitrate turnover in undisturbed coniferous forests. *Nature*, **385**, 61–64.

Swank WT, Vose JM (1997) Long-term nitrogen dynamics of Coweeta forested watersheds in the Southeastern United States of America. *Global Biogeochemical Cycles*, **11**, 657–671.

Thornton PE, Lamarque J, Rosenbloom NA, Mahowald NM (2007) Influence of carbon–nitrogen cycle coupling on land model response to CO_2 fertilization and climate variability. *Global Biogeochemical Cycles*, **21**, 1–15.

Valett HM, Thomas SA, Mulholland PJ *et al*. (2008) Endogenous and exogenous control of ecosystem function: N cycling in headwater streams. *Ecology*, **89**, 3515–3527.

Watmough SA, Eimers MC, Aherne J, Dillon PJ (2004) Climate effects on stream nitrate concentrations at 16 forested catchments in South Central Ontario. *Environmental Science and Technology*, **38**, 2383–2388.

Worrall F, Swank WT, Burt TP (2003) Changes in stream nitrate concentrations due to land management practices, ecological succession, and climate: developing a systems approach to integrated catchment response. *Water Resources Research*, **39**, 1–14.